Journal of Nuclear Materials 386–388 (2009) 152–156

Contents lists available at ScienceDirect

Journal of Nuclear Materials

journal homepage: www.elsevier.com/locate/jnucmat

Influence of damage rate on physical and mechanical properties and swelling of 18Cr–9Ni austenitic steel in the range of 3×10^{-9} to 4×10^{-8} dpa/s

E.N. Shcherbakov [a,*], A.V. Kozlov [a], P.I. Yagovitin [a], M.V. Evseev [a], E.A. Kinev [a], V.L. Panchenko [a], I. Isobe [b], M. Sagisaka [b], T. Okita [c], N. Sekimura [d], F.A. Garner [d]

[a] FSUE Institute of Nuclear Materials, Zarechny, Russia
[b] Nuclear Fuels Limited, Osaka, Japan
[c] University of Tokyo, Tokyo, Japan
[d] Pacific North-West National Laboratory, Richland, USA

A B S T R A C T

The results of the examination of the specimens constructed from the Fe–18Cr–9Ni steel thick-wall pipe irradiated at temperatures 370–375 °C to damage rates from 1.5 to 21 dpa at displacement rates from 3×10^{-9} to 4×10^{-8} dpa/s are presented. Electrical resistance, elasticity characteristics and radiation swelling of this material under different irradiation conditions were measured. Changes in the microstructure of the steel, in particular, the porosity characteristics dependent on a damage rate are shown.

1. Introduction

Numerous data on the influence of neutron irradiation on mechanical properties and dimensional stability were generated at high neutron flux levels in fast reactors. Many fission and fusion components operate at much lower displacement rates. Much less data are available for long-lived structural components operating at low neutron flux levels. In addition, most published data were generated from relatively thin specimens (~1–2 mm or less), while some actual structural components can be of the order of 10–20 mm. In this study, we examined a 95 cm external diameter pipe, 20 mm thick, constructed from Fe–18Cr–9Ni steel analogous to AISI 304L. The pipe operated under temperatures of 370–375 °C [1] in the BN-600 reactor, in a position outside the core, for 22 years. The pipe walls were sectioned into fragments to get specimens at a number of positions to yield doses in the range 1.5–22 dpa and at 3×10^{-9}–4×10^{-8} dpa/s.

2. Examination procedures

- 4 fragments were cut from the pipe:
- # 1 – the bottom of the pipe (BP);
- # 2 – the area deposed at a level of the core bottom (CB);
- # 3 – the area deposed at a level of the core centre (CC);
- # 4 – the area deposed at a level of the core top (CT);

The fragments # 2 and # 4 had only slight difference in neutron flux characteristics. Therefore, we selected the fragments ## 1, 2 and 3 for our examinations. Later two segments were cut with a diamond-milling machine remotely in a hot cell from every fragment. So we had 6 segments. Then we prepared a lot of specimens from each segment. A specimen had a dimension of $\sim 2 \times 4 \times 30$ mm, Fig. 1. Specimens that were cut from two segments from the first fragment were combined into one lot, because changes in a calculated achieved damage dose of the specimens did not exceed ±0.2 dpa. Other specimens of each segment were compounded into a separate lot. Specimens of the same lot had close irradiation conditions, Table 1.

The chemical composition of the pipe material is shown in Table 2, which also includes the comparison of the composition of three Fe–18Cr–9Ni steels: Fe–18Cr–9Ni (made in Russia) and AISI 304L (made in Japan and USA) as determined in the specifications [2].

Radiation-induced changes of electrical resistivity were measured by the electrical potential technique [3], Young's and shear moduli were measured by the resonance technique [3]. A relative instrumentation measurement uncertainty in both cases was within ±0.5%. In each lot, a density of two specimens was measured and the data generated were used to calculate radiation swelling with an absolute uncertainty being ±0.2 %. Then foils were prepared from the specimens of each lot to study microstructure by the transmission electron microscopy. In particular, porosity characteristics and second phase precipitates were determined.

In addition, electrical resistance, elasticity characteristics and density were measured for unirradiated specimens that were constructed from a thick steel plate fabricated from the same melt as the examined pipe.

* Corresponding author.
E-mail address: sfti@uraltc.ru (E.N. Shcherbakov).

0022-3115/$ - see front matter © 2009 Published by Elsevier B.V.
doi:10.1016/j.jnucmat.2008.12.080

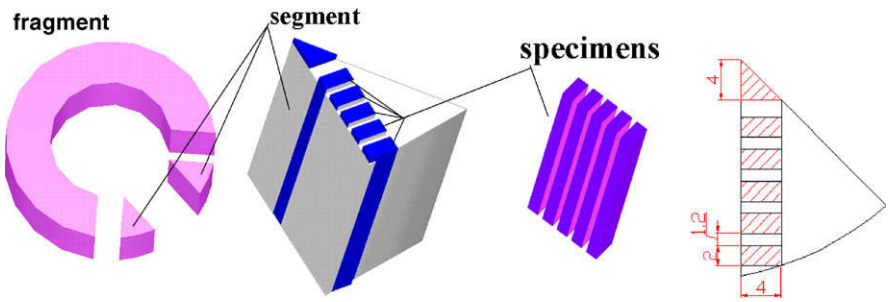

Fig. 1. The scheme of specimens cutting.

Table 1
Irradiation characteristics of examined specimens.

Specimen lot #	Damage rate (dpa)	Temperature (°C)	Displacement rate (dpa/s)
1	1.7 ± 0.2	372 ± 1	$(3.8 \pm 0.4) \times 10^{-9}$
2	9.9 ± 0.3	373 ± 1	$(2.10 \pm 0.04) \times 10^{-8}$
3	12.4 ± 0.3	375 ± 1	$(2.60 \pm 0.06) \times 10^{-8}$
4	16.2 ± 0.3	373 ± 1	$(3.40 \pm 0.06) \times 10^{-8}$
5	20.5 ± 0.4	376 ± 1	$(4.30 \pm 0.08) \times 10^{-8}$

3. Results

The measurement data on the electrical resistivity of the specimens in each lot were averaged. A dependence of a relative electrical-resistivity change (as compared to the unirradiated condition) of the examined steel on the damage rate is shown in Fig. 2. In this figure the instrumentation uncertainty intervals are designated on the curve about each measuring point. It is seen that a size of the changes is small (<2%) and a manner of their dependence on the exposure dose is mainly nonmonotonic.

Dependence of the relative change in Young's modulus is shown in Fig. 3. It is characterized by practically monotonic decrease in Young's modulus with dose growth. We note that statistical mean square errors (MSEs) in the determination of the average values of the electrical resistance of the specimens in lot #3 and elasticity modulus of the specimens in lot #5 are higher than the value associated with the instrumentation uncertainty shown in Table 3.

The dependence of swelling on an exposure dose derived from the density data is shown in Fig. 4. Swelling increases with the exposure dose and is well approximated with a square function.

The electronic microscopy revealed voids in all irradiated specimens. In Table 4 the average sizes and concentrations of the voids in the specimens irradiated to different damage rates as well as the swelling values estimated from histograms of a void size distribution are presented as referred to Fig. 5(a), (c)–(f). It is seen that the concentrations of the voids in the specimens irradiated to different damage rates (this difference is about an order of magnitude) have close values, and the mean radius of the voids increases monotonously with the damage rate. The voids in the specimens irradiated

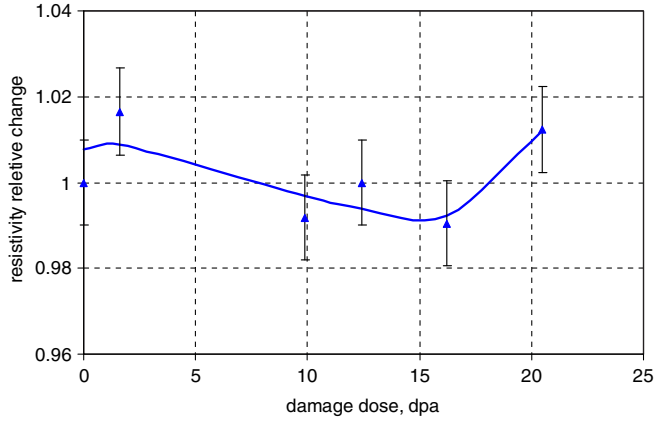

Fig. 2. Dependence of relative change in electrical resistivity of Fe–18Cr–9Ni steel on neutron irradiation dose.

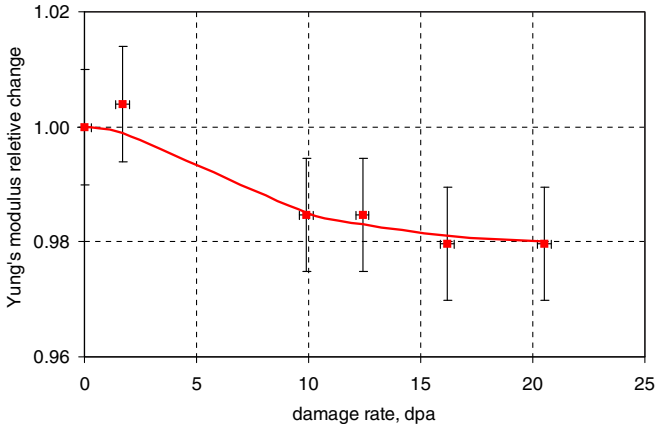

Fig. 3. Dependence of relative change in Young's modulus of Fe–18Cr–9Ni steel on neutron irradiation dose.

Table 2
Chemical composition of Fe–18Cr–9Ni steels produced in Russia, Japan and USA.

Alloying agent composition, mass% Pipe material composition (certificate data)								
C	Mn	Si	P	S	Ni	Cr	Cu	Fe
0.09	1.36	0.38	0.025	0.020	8.75	17.66	0.21	Balance
Fe–18Cr–9Ni (17X18H9, Russia)								
0.13–0.21	<2.0	<0.8	<0.03	<0.02	8.0–10.0	17.0–19.0	<0.2	Balance
AISI 304L (Japan, USA)								
<0.03	<2.0	<1.0	<0.04	<0.03	8.0–13.0	18.0–20.0	–	Balance

Table 3
Average values of electrical resistivity and Young's modulus and mean square errors (MSEs) used for their determination.

Lot #	Damage rate (dpa)	E (GPa)		ρ (10^{-8} Ohm m)	
		Average	MSE[a]	Average	MSE[a]
Unirradiated	0	202	1	72.9	0.5
1	1.7	203	1	74.1	0.4
2	9.9	199	1	72.3	0.4
3	12.4	199	*1*	72.9	*1.0*
4	16.2	198	1	72.2	0.4
5	20.5	198	*2*	73.8	*1.0*
MSE, allowed by instrumentation uncertainty			**0.1**		**0.4**

[a] MSE $= \sqrt{\frac{\sum_{i=1}^{n}(x_i-\bar{x})^2}{n\cdot(n-1)}}$ where i is the number designating a specimen in a lot; x_i, the value obtained for the specimen; $\bar{x}$, the average value; and n, the quantity of the specimens in a lot (4 or 5 for different lots).

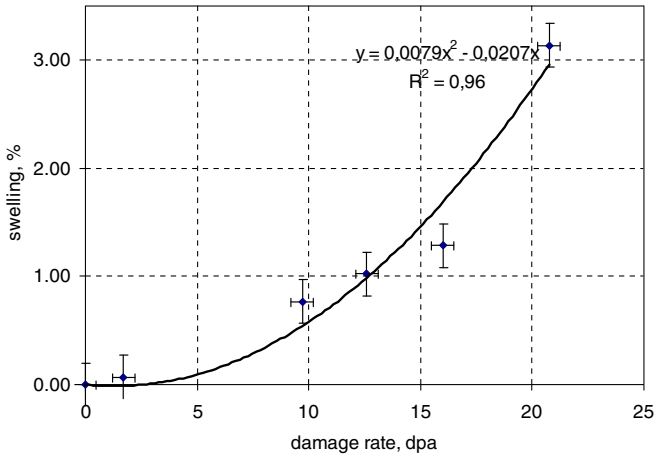

Fig. 4. Damage rate dependence of swelling derived from density measurement data.

Table 4
Average sizes and concentrations of voids in specimens irradiated to different damage rates.

Lot #	Damage dose (dpa)	Average size of voids (nm)	Concentration of voids (10^{21} m^{-3})	Swelling (%)
1	1.7	10	4.1	0.25
2	9.9	13	5.2	1.00
3	12.4	14	5.0	0.95
4	16.2	17	4.1	1.60
5	20.5	19	5.8	2.30

to a minimum damage rate (1.7 dpa) are small, practically they are not related to precipitates, Fig. 5b. Their relation to dislocation structure elements is traceable. A quantity of voids associated with second phase precipitates is growing with the damage rate. An appearance of such voids irradiated to 20.5 dpa is shown in Fig. 5(h). Judging by the microdiffraction analysis data it appears to be G-phase though its lattice parameter is smaller than normally G-phase has. This phase usually forms during the irradiation of Ti-bearing steel.

Phases of other sort that form mainly along grain boundaries are carbides M_6C and $M_{23}C_6$. Besides, quite extended areas of α-phase were observed to form in γ-crystalline matrix. Such area in the specimen irradiated to 20.5 dpa is shown in Fig. 5(g).

4. Discussion

The examination showed that at temperatures 370–375 °C and at displacement rates 3×10^{-9}–4×10^{-8} dpa/s radiation swelling of Fe–18Cr–9Ni occurs even at several units of dpa and at ~20 dpa its value reaches about 3%. In addition to this, there are other structural changes that contribute to the final change in electrical resistance and elasticity characteristics. It is shown in [4] that provided there are no other structural changes or when a swelling contribution makes a dominating effect on physical and mechanical properties, the swelling-induced changes in the electrical resistance and Young's modulus can be calculated from the formulas

$$\frac{\Delta R}{R_0}=\frac{5\cdot S}{4\cdot S+6}, \tag{1}$$

$$\frac{\Delta E}{E_0}=\frac{1}{(1+S)^2}-1, \tag{2}$$

where ΔR and ΔE are the absolute changes in electrical resistance and Young's modulus, respectively;

R_0 and E_0 are the electric resistance and Young's modulus of the initial condition of the material, respectively;

S is the swelling represented in unit parts.

We use Eqs. (1) and (2) to compare the changes in the physical and mechanical properties of the steel after irradiation to different damage rates and an onset of swelling. For this comparison, R/R_0 and E/E_0 were calculated as based on swelling data. The swelling data were obtained by the hydrostatic technique and electron microscopy. The calculation ratios R/R_0 and E/E_0 were compared with the data shown in Figs. 6 and 7.

The available experimental data of relative changes in electrical resistance are differed on one to two intervals of mean square error.

This is evidence of significant effect of other factors. This is testified that some other factors are affected significantly on changes in electrical resistance. These factors include changes in the chemical composition of the matrix, such as the content of substitutional impurities and the formation of second phases proceeding along with a simultaneous change in a crystalline matrix composition. The observed formation of the carbides on grain boundaries causes a reduction of carbon atoms in a solid solution, which would lead to a decrease in the relative electrical resistance [5].

In the unirradiated condition of the material there are not many carbides in grains, there are no second phase precipitates on the grain boundaries. After irradiation one can see many carbides on the grain boundaries. In some cases, carbides generate layers in the specimens irradiated to doses above 15 dpa.

Observed by electron-microscopic examination the formation of α-phase characterized itself by minor both relative electrical resistance and Young's modulus would also lead to a decrease in the electrical resistance.

The dependence of relative change in Young's modulus on damage dose calculated by measured values of swelling is in good agreement with the experimental values up to a dose of

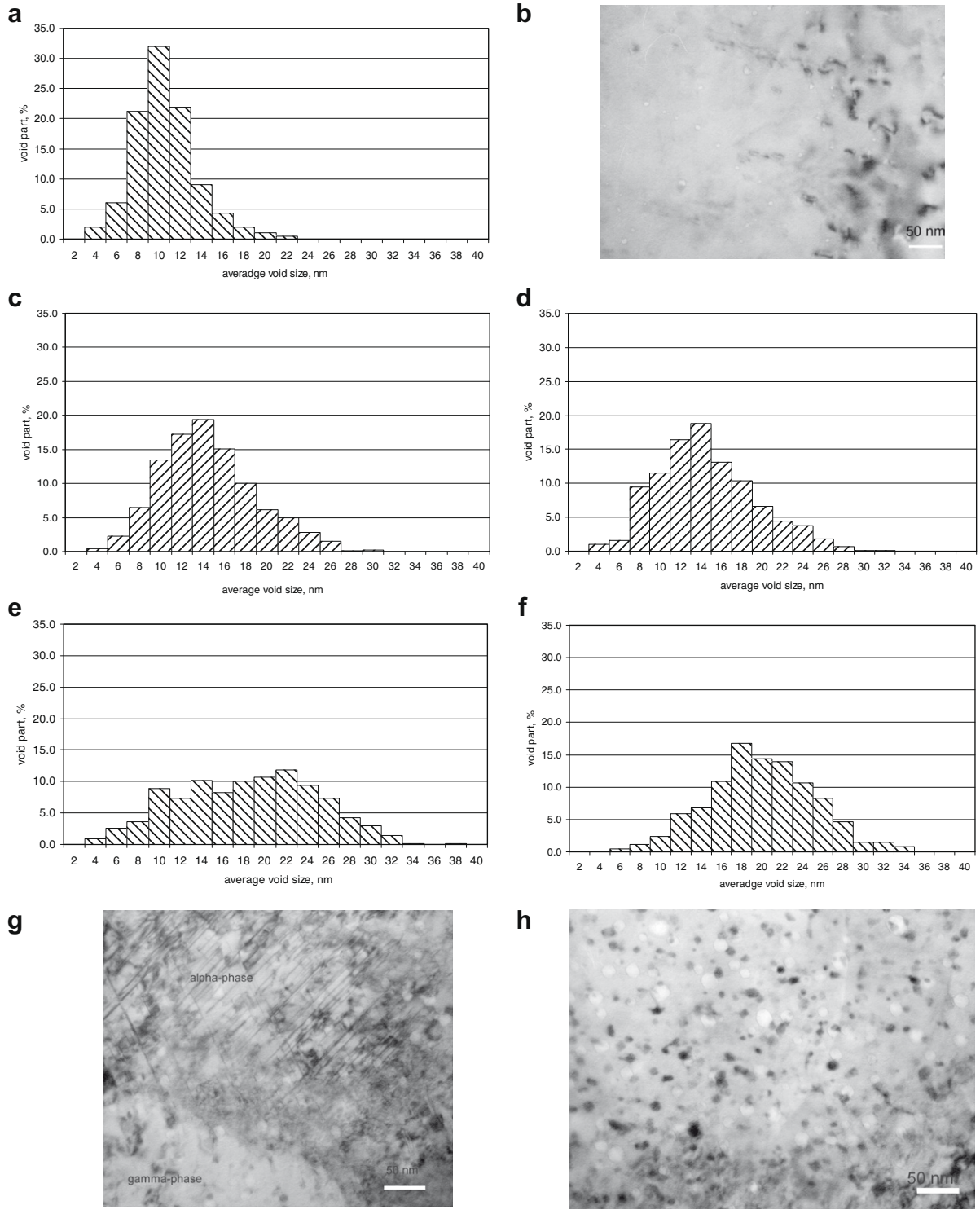

Fig. 5. Results of the examination of Fe–18Cr–9Ni steel specimens microstructure: a, c, d, e, f – histograms of void size distribution in specimens irradiated to doses 1.7; 9.9; 12.4; 16.2 and 20.5 dpa; b – voids after irradiation to 1.7 dpa; h – voids after irradiation to 20.5 dpa; g – area of α-phase in γ-crystalline matrix.

16 dpa (Fig. 7). The measured values of Young's modulus are higher than the calculated values at 20.3 dpa. The reduction of carbon concentration in the matrix due to its transfer into carbides and passage to grain boundaries may be the cause of such a difference [5].

A high discrepancy in the properties within the same lot and hence a deviation of the average values might be due to the inhomogeneity of the pipe material since the examined specimens were cut out of the true commercial thick-metal structure. As is known it is more difficult to provide a uniformity of a material structure and composition by a commercial fabrication than by a special production of specimens from laboratory melts. In order to estimate the degree of chemical homogeneity, the specimens from different lots were checked for Ni, Cr and Si contents by the X-ray microdiffraction analysis. In total, seven specimens were analyzed, four or five times each, the area for one run was

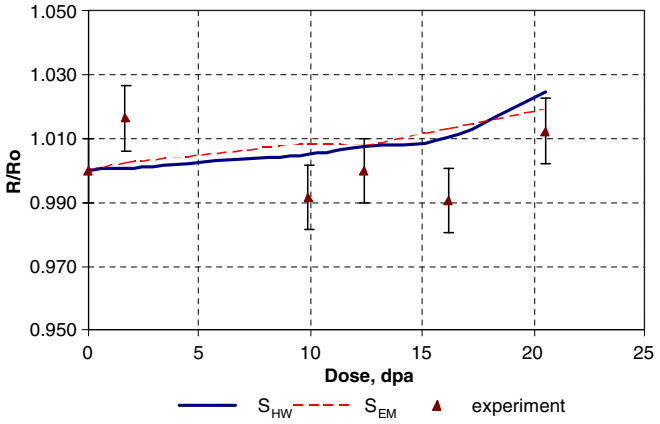

Fig. 6. The verification results of experimentally derived changes in specific electrical resistivity (plotted points) and swelling-induced change (the solid curve – swelling S_{HW} measured by the hydrostatic weighing procedure; the dotted curve – swelling S_{EM} obtained by the electron microscopy procedure).

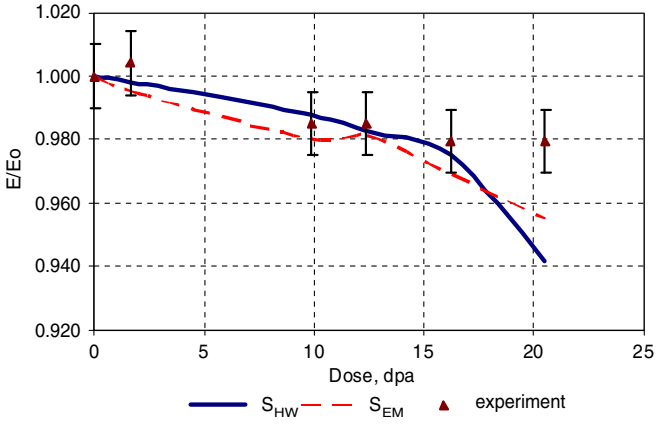

Fig. 7. The verification of experimentally derived data of relative changes in Young's moduli (points) with swelling-induced change (the solid curve – swelling S_{HW} measured by the hydrostatic weighing procedure; the dotted curve – swelling S_{EM} obtained by the electron microscopy procedure).

$\sim 50 \times 50\ \mu m^2$, later the data for each specimen were averaged. For different specimens, the content was as follows: Ni – 8.5–8.9%; Cr – 17.1–18.0%; Si – 0.9–1.1%.

Unfortunately, we have a small unirradiated sample of ingot of the same casting material as the tested pipe. It did not permit to estimate inhomogeneity in the removed from each other areas of the long-length pipe. Therefore, we can neither confirm, nor deny the assumption of influence of initial inhomogeneity as one of the reasons of observable disorder of properties in various lots of specimens.

The scattering of the data on the structure and properties in the same lot can be associated with the gradients of temperatures and stresses along the cross-sections at different positions of the thick-wall construction, the actual values of which may differ from those generated from simulated thermal calculations of γ-heating and heat removal at the positions of the pipe wall during its operation in the reactor.

In order to consider the effect of other structural factors on the relation of the changes in the physical and mechanical properties with swelling it is necessary to obtain data on evolution of the crystal matrix and second phases (in particular, α-phase), that can be provided by magnetometry and X-ray diffraction analysis.

5. Conclusions

- Irradiation of the Fe–18Cr–9Ni austenitic steel thick-wall pipe at 370–375 °C to damage rates from 1.5 to 21 dpa at displacement rates from 3×10^{-9} to 4×10^{-8} dpa/s resulted in radiation swelling about 3%.
- The changes in the electrical resistance and elasticity characteristics occurred during ~130 000 h show complex dependence on the damage rate; a maximum size of the relative changes of the electrical resistivity and Young's modulus was not more than 2% of the corresponding values for the material in its initial condition.
- In addition to the radiation swelling there are other factors that make significant contribution under the realized irradiation conditions on the physical and mechanical properties; these factors are the formation of the second phases (carbides, G-phase and α-phase) and the changes in the composition of the crystalline matrix.
- For a correct prediction of the changes that occurred under the long-term neutron irradiation, the changes of the physical and mechanical properties of the Fe–18Cr–9Ni type steel, it is necessary to conduct a detailed study of the structural changes by using magnetometry and the X-ray diffraction analysis.

References

[1] B.Z. Margolin, A.I. Minkin, V.I. Smirnov, V.A. Fedorova, V.I. Kokhonov, A.V. Kozlov, M.V. Evseev, E.A. Kozmanov, Prob. Strength Plast., in press (in Russian).
[2] M.I. Goldshtein, S.V. Grachev, G. Veksler Yu, Special Application Steels, Metallurgia, Moscow, 1985 (in Russian).
[3] E.B. Averin, I.M. Kostousov, E.V. Serovikova, E.N. Shcherbakov, Nucl. Eng. Technol. 3 (1992) 43 (in Russian).
[4] A.V. Kozlov, E.N. Shcherbakov, S.A. Averin, F.A. Garner, in: M.L. Grossbeck (Ed.), 21st International Symposium, ASTM STP 1447, ASTM International, West Conshohocken, PA, 2003.
[5] B.G. Lifshits, V.S. Karposhin, L. Linetskii Ya, Physical Properties of Metals and Alloys, Metallurgia, Mosocow, 1980 (in Russian).